Food Research International 206 (2025) 116048

Contents lists available at ScienceDirect

Food Research International

journal homepage: www.elsevier.com/locate/foodres

Adsorption properties of molecularly imprinted polymers designed for removal of smoke taint compounds from wine

Yiming Huo [a], Renata Ristic [a], Maxime Savoie [b], Richard Muhlack [a,*], Markus Herderich [a,c], Kerry Wilkinson [a]

[a] Discipline of Wine Science and Waite Research Institute, The University of Adelaide, PMB 1, Glen Osmond, SA 5064, Australia
[b] amaea LP, 10 Bisley Road, Hamilton, 3214, New Zealand
[c] The Australian Wine Research Institute, PO Box 197, Glen Osmond, SA, 5064, Australia

ARTICLE INFO

Keywords:
Adsorption isotherm
Langmuir isotherm
Freundlich isotherm
Remediation
Smoke taint
Volatile phenols
Volatile phenol glycoconjugates

ABSTRACT

The presence of elevated concentrations of smoke-derived volatile phenols (and their glycoconjugates) in wine after grapevine exposure to wildfire smoke can give wine unpleasant smoky and ashy characters. To date, options for remediation of 'smoke taint' are limited, therefore, this study evaluated the potential for a commercially developed molecularly imprinted polymer (MIP) to remove smoke taint compounds from wine. A single-solute adsorption study was conducted in model wine and demonstrated adsorption of guaiacol, phenol and *m*-cresol by a diverse range of binding sites on the MIP surface. The adsorption capacity of the MIP towards guaiacol was estimated to be 1.2 μmol/g, with a higher capacity and affinity estimated for *m*-cresol (being 1.7 μmol/g). When a fixed-bed column packed with MIPs was used to treat smoke tainted Chardonnay, rosé and Cabernet Sauvignon wines the MIP column removed up to 47 % of the volatile phenols present in wine (but not volatile phenol glycoconjugates), with no detrimental effect on wine colour density and phenolic composition. Experiments evaluating column break-through and the reusability of MIPs were also performed to further establish the application potential of MIPs for remediation of smoke taint in wine.

1. Introduction

Since its large scale production during the Neolithic period (ca. 5400–5000 BCE), wine has become a popular beverage around the world (Estreicher, 2017), and winemaking has become an important industry sector in many countries.

As with the production of other beverages (e.g., water, dairy, juice, beer, cider), quality control is crucial in wine production. Various faults and taints have been identified by winemakers and consumers, including protein haze (Waters et al., 2005), cork taint (Pereira et al., 2000; Sefton & Simpson, 2005), oxidation (Oliveira et al., 2011), ladybug taint (Pickering & Botezatu, 2021), *Brettanomyces* spoilage (Chatonnet et al., 1992), and more recently, smoke taint (Kennison et al., 2007; Ristic et al., 2016).

Smoke taint arises due to vineyard exposure to bushfire/wildfire smoke, whereby smoke-derived volatile compounds, including volatile phenols (Table S1), can be taken up by grapevine leaves and fruit, after which they accumulate in bound forms, i.e., as glycoconjugates (Dungey et al., 2011; Hayasaka et al., 2010a; Hayasaka et al., 2010b; Noestheden et al., 2018). Smoke-derived volatile phenols (i.e., guaiacol, 4-methylguaiacol, phenol, *o*-, *m*-, and *p*-cresol, syringol and 4-methylsyringol) can be extracted (in free and glycosylated forms) during fermentation (Kennison et al., 2009; Ristic et al., 2016), resulting in smoky, burnt rubber, medicinal and ashy characters in wine (Hayasaka et al., 2013; Parker et al., 2012).

Smoke-tainted wines are typically rejected by consumers, even after considerable dilution (Bilogrevic et al., 2023), thus winemakers and researchers alike are attempting to solve the problem. Many of the strategies evaluated for mitigating smoke contamination of grapes in the vineyard (Favell et al., 2019; Favell et al., 2021; Wilkinson et al., 2022) have limited efficacy and/or are logistically not feasible, whereas winemaking techniques at best only partially mitigate the sensory expression of smoke taint (Ristic et al., 2011). Some adsorbents have been found to be effective at removing smoke taint compounds from

Abbreviations: MIP, molecularly imprinted polymer; NIP, non-imprinted polymer; ANOVA, analysis of variance; GC–MS, gas chromatography–mass spectrometry; HPLC-MS/MS, high performance liquid chromatography-tandem mass spectrometry; RATA, rate-all-that-apply..

* Corresponding author.
E-mail address: richard.muhlack@adelaide.edu.au (R. Muhlack).

https://doi.org/10.1016/j.foodres.2025.116048
Received 18 November 2024; Received in revised form 27 January 2025; Accepted 21 February 2025
Available online 23 February 2025

wine, but often, desirable compounds were also removed during treatment (Culbert et al., 2021; Fudge et al., 2012). Alternative approaches to remediation are therefore sought; both the use of more selective adsorbents (Dang et al., 2020; Huo et al., 2024) and their use in combination with separation technologies (Fudge et al., 2011; Puglisi et al., 2022), to better address smoke taint in the winery.

Molecularly imprinted polymers (MIPs) are synthetic adsorbents designed around specific target compounds and they have long been used in food and beverage applications (BelBruno, 2019; Cengiz et al., 2022; Murray & Örmeci, 2012; Sellergren & Hall, 2012; Vasapollo et al., 2011). The preparation of MIPs initially involves the addition of functional monomers and target compounds (or their analogues) as templates. After polymerisation, removal of the template leaves specific binding sites within the polymer matrix (Fig. 1). The specificity of MIP binding sites enables their selective adsorption of target compounds (Liu et al., 2022), as well as their reuse, after an appropriate regeneration process (Liang et al., 2018b; Söylemez et al., 2021). Non-imprinted polymers (NIPs) are counterparts to MIPs, and they are synthesized in the same manner, but without template molecules. Studies have confirmed the successful imprinting and selective adsorption of MIPs compared with NIPs (Chen et al., 2013; Filipe-Ribeiro et al., 2020; Söylemez et al., 2021).

The mechanism of adsorption is a crucial question in the development and assessment of novel sorptive materials, and isotherm studies enable characterisation of adsorption properties (Foo & Hameed, 2010). The present study sought to evaluate the adsorption properties of a commercially produced MIP and its capacity to remove free and glycosylated volatile phenols from wine, as a novel approach to remediation of smoke taint.

2. Theory

Binding sites on the surfaces of adsorbents can be classified (according to their shape, size, the depth of their cavities and the uniformity of their binding energy or adsorption affinity) as homogeneous or heterogeneous (Umpleby II et al., 2000; 2004). A homogeneous surface is considered uniform where binding sites have the same binding energy (Ayawei et al., 2017), whereas a heterogeneous surface is characterised by variation in binding energies (affinity) and selectivity (Umpleby II et al., 2004). Molecules can also bind to the surface of adsorbents in single or multiple layers, forming mono- and multi-layer adsorptions (García-Calzón & Díaz-García, 2007).

Adsorption isotherm models have been developed to describe and characterise the interactions between target adsorbates and the liquid-solid interface of adsorbents (Foo & Hameed, 2010). Linear forms of several key adsorption models are summarized in Table 1. Individual models have different assumptions regarding the recognition of target compounds by the binding sites on the surface of adsorbents. The agreement of experimental data with isotherm models provides insight into the adsorption properties of adsorbents and an understanding of their recognition mechanism and adsorption behaviors. Isotherms have therefore become valuable tools in the evaluation of adsorbent properties and performance (Ateia et al., 2020; Foo & Hameed, 2010).

Langmuir is one of the most widely used isotherm models, and assumes monolayer adsorption by homogeneous binding sites that are distributed on the surface of the adsorbents (Abu-Alsoud et al., 2020; Langmuir, 1918). Binding energies on the surface are assumed to be consistent with no transmigration of adsorbate on the surface (Langmuir, 1918; Saadi et al., 2015). Bi-Langmuir and other higher-order Langmuir models assume relatively homogeneous surfaces, where two or more distinct classes of binding sites are proposed (Umpleby II et al., 2000; 2004).

Temkin analysis can fit adsorptions where there are indirect adsorbate/adsorbent interactions based on uniform binding energy, up to some maximum binding energy, where binding energy decreases linearly with an increasing amount of adsorbates on the surface (Johnson & Arnold, 1995; Víctor-Ortega et al., 2016).

Brunauer-Emmett-Teller (BET) theory is based on a homogeneous surface with no interaction between solute molecules. It starts with single layer adsorption but can be extended to multilayer adsorption system if adsorbed molecules offer binding sites (Abu-Alsoud et al.,

Table 1
Adsorption isotherm models.

Isotherm	Equation		Plot
Langmuir[a]	$\frac{1}{Q_e} = \frac{1}{Q_{m-L}} + \frac{1}{bQ_{m-L}}\frac{1}{C_e}$	Q_e (μmol/g): adsorbate adsorbed at equilibrium C_e (μmol/L): adsorbate concentration at equilibrium Q_{m-L} (μmol/g): adsorption capacity of adsorbent b (L/μmol): Langmuir adsorption equilibrium constant	$\frac{1}{Q_e}$ Vs $\frac{1}{C_e}$
Freundlich[b]	$logQ_e = logK_F + n_F logC_e$	$K_F[(\mu mol/g)\ (L/\mu mol)^{n_F}]$: adsorption capacity n_F: surface heterogeneity	$logQ_e$ Vs $logC_e$
Halsey[c]	$lnQ_e = \frac{1}{n_H}ln K_H + \frac{1}{n_H}lnC_e$	K_H $[(\mu mol/g)\ (L/\mu mol)^{n_H}]$: Halsey model constant n_H: Halsey model exponent	lnQ_eVs lnC_e
Temkin[d]	$Q_e = E_T ln(K_T C_e)$	$E_T(J/kg)$: heat of sorption $K_T(L/kmol)$: Temkin constant	Q_eVs lnC_e
Dubinin-Radushkevich (D-R)[e]	$lnQ_e = ln Q_{m-DR} - K_{D-R}\varepsilon^2$ $\varepsilon = RTln\left(1 + \frac{1}{C_e}\right)$ $E_{DR} = (2K_{DR})^{-1/2}$	K_{DR} (KJ^2/mol^2): Dubinin-Radushkevich constant ε: Polanyi potential E_{DR} (kJ/mol): mean adsorption energy Q_{m-DR} $(\mu mol/g)$: adsorption capacity of adsorbent R: gas constant $(8.314\ J/mol/K)$ T (K): absolute temperature	lnQ_e Vs ε^2
Scatchard plot[f]			Q_e/C_e Vs C_e

[a] refers to (Abu-Alsoud et al., 2020; Langmuir, 1918; Saadi et al., 2015).
[b] refers to (Abu-Alsoud et al., 2020; Ayawei et al., 2017; Sips, 1948).
[c] refers to (Liu & Wang, 2013; Shahnaz et al., 2020).
[d] refers to (Johnson & Arnold, 1995; Liu & Wang, 2013; Víctor-Ortega et al., 2016).
[e] refers to (Liang, Jeffery and Taylor, 2018b; Liu & Wang, 2013).
[f] refers to (Abu-Alsoud et al., 2020; Umpleby II et al., 2004).

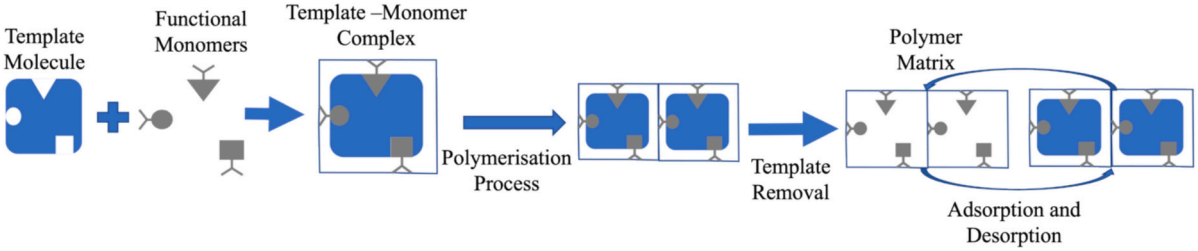

Fig. 1. Schematic of molecular imprinting technology.

2020; Foo & Hameed, 2010).

The **Dubibin-Radushkevich (D-R)** model was developed to estimate the porosity of adsorbent beads and the Gaussian energy distribution of (monolayer) adsorption on a heterogeneous surface and the model has been widely used to differentiate the physical and chemical adsorption of the adsorbates (Ayawei et al., 2017; Liang et al., 2018b; López et al., 2012).

The **Freundlich** isotherm has been widely used for describing adsorption on heterogeneous surfaces by adsorbents whose binding energies are distributed exponentially, with a high likelihood of multilayers forming (Freundlich, 1906; Sips, 1948).

The **Hasley** model takes into account multilayer adsorption at relatively large distances from the surface, and alignment with Hasley might confirm the heterogeneity of an adsorbent's binding sites (Saadi et al., 2015; Shahnaz et al., 2020).

Langmuir-Freundlich isotherm **(L-FI)** is a hybrid of two basic isotherms, which reduces to the Freundlich equation at low concentrations and to the classic Langmuir at high concentrations of the analyte. L-FI is characterised by the ability to model both saturation and sub-saturation behaviors (Abu-Alsoud et al., 2020; Sips, 1948).

3. Materials and methods

3.1. Chemicals

Analytical grade solvents (ethyl acetate, pentane, dichloromethane and ethanol) were purchased from Merck (Truganina, Vic., Australia), while volatile phenols (guaiacol, 4-methylguaiacol, phenol, *o*-, *m*-, and *p*-cresol, syringol, and 4-methylsyringol) were purchased from Sigma Aldrich (Castle Hill, NSW, Australia). Analytical grade reagents (sodium hydroxide, potassium hydrogen tartrate (KHT), anhydrous citric acid, and sodium carbonate) were purchased from Rowe Scientific (Lonsdale, SA, Australia). Food grade 96 % ethanol was purchased from Tarac Technologies (Nuriootpa, SA, Australia).

Isotopically labelled internal standards were either synthesized in-house (d_4-guaiacol) as previously reported (Crump et al., 2014; Szeto et al., 2022), or purchased from LGC Standards (Manchester, NH, USA; d_3-syringol, d_5-*o*-cresol, d_6-phenol and d_6-syringol gentiobioside).

3.2. Molecularly imprinted polymers

The MIPs used in this study were supplied by amaea (Hamilton, NZ) and ranged in size from 0.3 to 3.0 mm; their preparation is proprietary and non-imprinted polymers were not available for comparison.

MIPs were conditioned prior to use in adsorption experiments by soaking in 15 % aqueous ethanol (3 times, 30 min each) according to manufacturer instructions, as previously reported (Huo et al., 2024). Column-packed MIPs were similarly conditioned, and also regenerated after use, following manufacturer instructions, i.e.: for conditioning, two bed volumes (BVs) of 15 % aqueous ethanol were eluted; while for regeneration, two BVs of 15 % aqueous ethanol, five BVs of neat (96 %) ethanol, and then two further BVs of 15 % aqueous ethanol were eluted; all flow rates were ~ 15–20 BV/h (Table 2).

Table 2
Operating parameters for MIP treatment of smoke tainted Chardonnay, Cabernet Sauvignon and rosé wines.

Wine	MIP mass (g)	MIP bed volume (L)	Flow rate (BV/h)	
			During treatment	During regeneration
Chardonnay	700	2.00	42.6	21.3
Cabernet Sauvignon	1000	2.86	28.4	14.2
Rosé	1000	2.86	28.4	14.2

3.3. Adsorption of volatile phenols by MIPs from model wine (isotherm experiment)

To model the adsorption of volatile phenols by MIPs, a single solute adsorption study was conducted in model wine (in triplicate). Various quantities of MIPs (1 to 10 g/L) were added to model wine (i.e., 12 % aqueous ethanol, saturated with potassium hydrogen tartrate, and pH adjusted to 3.4), spiked with guaiacol, phenol and *m*-cresol to achieve a gradient ratio of adsorbate to adsorbent of 1–500 μg/g per L of model wine. The removal of volatile phenols due to adsorption by MIPs was determined by comparing the guaiacol, phenol and *m*-cresol concentrations (measured by gas chromatography–mass spectrometry (GC–MS) analysis, as described below) in model wine before and after MIP addition (for 48 h with mixing, using an orbital shaker (Retek, Boronia, Vic., Australia)).

3.4. Adsorption of volatile phenols by MIPs from smoke tainted wine (remediation experiment)

Smoke tainted Chardonnay, Cabernet Sauvignon and rosé wines (made from grapes harvested from vineyards (in New South Wales, Australia) that were exposed to smoke from fires that burned during the 2019–2020 grape growing season) were treated at semi-commercial scale (in duplicate) by sequential elution through MIP-packed column (Table 2); i.e., 160 L of each wine (Chardonnay, then Cabernet Sauvignon, then rosé) was passed through the column for each replicate. Preliminary analysis of volatile phenols and their glycoconjugates (Tables S2 and S3), measured as described below, indicated the Chardonnay and Cabernet Sauvignon wines were more heavily tainted than the rosé wine. As such, Chardonnay and Cabernet Sauvignon wines were each eluted two times, with two BVs of 15 % aqueous ethanol, five BVs of 96 % ethanol and two BVs of 15 % aqueous ethanol eluted between MIP treatment of different wines; while two BVs of 15 % aqueous ethanol were eluted before the second pass of Chardonnay; and two BVs of 15 % aqueous ethanol, two BVs of 96 % ethanol and two BVs of 15 % aqueous ethanol eluted between passes of Cabernet Sauvignon. The less tainted rosé wine was eluted only once. The flow rates and BVs for each MIP treatment are detailed in Table 2. During treatment, 20 L fractions were collected and sub-sampled for chemical analysis, before being blended. Treated wines were bottled (in 750 mL glass bottles under screw cap) for chemical and sensory analysis, along with untreated wines, approximately 2 months post-bottling.

3.5. Chemical analysis of wine

3.5.1. Analysis of wine colour and phenolics

The colour of red and rosé wines was measured using the Somers assay (Mercurio et al., 2007) with an Infinite 200® PRO spectrophotometer (Tecan, Männedorf, Switzerland). Total phenolics and browning were measured in Chardonnay wines (as absorbance at A280 and A420 nm, respectively (Ortega et al., 2003; Sims et al., 1995)), using the same spectrophotometer.

3.5.2. Analysis of volatile phenols and volatile phenol glycoconjugates

The concentration of volatile phenols (guaiacol, 4-methylguaiacol, phenol, *o*-, *m*-, *p*-cresol, syringol and 4-methylsyringol) were measured in wine and model wine samples using an Agilent 6890 gas chromatograph equipped a 5973 mass spectrometer (Agilent Technologies, Forest Hill, Victoria, Australia), following previously published stable isotope dilution assay methods (Hayasaka et al., 2013; Pollnitz et al., 2004). The internal standards used for quantitation were d_4-guaiacol, d_3-syringol, d_5-*o*-cresol and d_6-phenol. Instrumental conditions were consistent with previous studies (Hayasaka et al., 2013), and MassHunter and ChemStation (version B.04.03, Agilent Technologies) were used for data acquisition and processing.

Volatile phenol glycoconjugates were measured in wine samples (as

syringol gentiobioside equivalents) using an Agilent 1200 high-performance liquid chromatograph equipped with a 1290 binary pump, coupled to an AB SCIEX Triple Quad 4500 tandem mass spectrometry with a Turbo V ion source (Framingham, MA, USA) again using published stable isotope dilution assays (Hayasaka et al., 2010a, 2013). Sample preparation and instrumental parameters were consistent with previous research (Hayasaka et al., 2010a, 2013), with d_6-syringol gentiobioside used as the internal standard. Analyst software (version 1.7 AB SCIEX) was used for data acquisition and processing. The limits of quantitation for both volatile phenols and volatile phenol glyco-conjugates were 1 μg/L.

3.6. Sensory analysis of wine

The sensory profiles of control wines and treated Chardonnay, Cabernet Sauvignon and rosé wines were determined (in duplicate) approximately two months after bottling, using the Rate-All-That-Apply (RATA) method (Ares et al., 2014), and a panel comprising regular wine consumers (n = 53, aged between 22 and 80 years, 16 males and 47 females). Wines (30 mL) were served in covered, 4-digit coded 315 mL transparent stemmed glasses, in a randomised order across participants. Before tasting, panelists were introduced to the RATA procedure and a list of sensory attributes adapted from previous studies (Huo et al., 2024; Ristic et al., 2015). Sensory evaluations were completed in a purpose-built sensory laboratory under controlled conditions: i.e., at between 22 and 24 °C, under white sodium lights. Between samples, panelists rested for at least 60 s, with water and plain crackers provided as palate cleansers.

Sensory data were acquired with Red Jade software (Redwood Shores, CA, USA). Panelists gave informed consent before participating in the study, which was approved by the Human Research Ethics Committee of the University of Adelaide (Ethics Approval Number. H-2021-175).

3.7. Data analysis

Chemical data were analysed by one-way analysis of variance (ANOVA), with mean comparisons conducted by HSD post hoc test at $p < 0.05$, using XLSTAT (version 2022, Lumivero, New York, USA). Sensory data were analysed by two-way ANOVA (with participants as a random factor and wines as a fixed factor) and LSD post hoc test at $p < 0.05$ to determine significant differences between wines at $p < 0.05$ using SenPAQ software (v6, Qi statistic, UK).

4. Results and discussion

4.1. Adsorption of volatile phenols by MIPs in a model wine matrix

To study the adsorption of smoke-derived volatile phenols by MIPs, an adsorption study was conducted in model wine, spiked with different concentrations of guaiacol, phenol or *m*-cresol. The resulting data were studied using various isotherm models to characterise MIP adsorption behavior and gain insight into likely adsorption mechanics/kinetics.

Considering the concentration of volatile phenols in smoke tainted wine is usually relatively low (i.e., < 100 μg/L) and their estimated detection thresholds are typically between 20 and 65 μg/L (Table S1), the analytical range targeted in the present study was 0 to 500 μg/L (for guaiacol, phenol and *m*-cresol).

4.1.1. Effect of initial concentration and MIP dose on adsorption

A recent study (Huo et al., 2024) demonstrated that adsorption-desorption equilibriums can be achieved in a wine matrix after 24 h of MIP contact (with mixing). Therefore, in the present study, treatments were applied over 48 h to ensure equilibrium was reached at the time of sampling.

The adsorbed quantity of each volatile phenol Q_e (μmol/g) was determined by the equation:

$$Q_e = \frac{(C_i - C_e)V}{m}$$

where C_i and C_e (μmol/L) are the initial and equilibrium concentrations of guaiacol, phenol or *m*-cresol; V (L) is the volume of each solution; m (g) is the mass of MIP beads added to solutions; and Q_e (μmol/g) is the amount of adsorbate at equilibrium.

When the amount of adsorbate/adsorbent was plotted against their initial concentration ratio (Fig. 2), it shows an initial increase in the ratio of adsorbate/adsorbent per volume of model wine matrix, up to ~1 μmol/g, i.e., the maximum adsorbed amount of each volatile phenol that can be achieved per mass of dry MIPs increased almost linearly. When the initial concentration ratio exceeded ~2 μmol/g/L, isotherm lines of volatile phenols were prone to plateau, indicating that the MIPs likely approached their adsorption capacities towards the different volatile phenols. As reported in an adsorption study by Víctor-Ortega et al. (2016), the removal efficiency of phenol by ion exchange resin decreased as the phenol load in water increased because of resin saturation; i.e., the resin achieved its adsorption capacity. The MIPs appeared to have a higher affinity towards *m*-cresol compared with guaiacol and phenol, as a higher Q_e(μmol/g) was observed for *m*-cresol regardless of solute concentrations. This might reflect the hydrophobicity of adsorbates (Table S1), as *m*-cresol is more hydrophobic (log P = 1.96). This observation supports findings from previous MIP adsorption experiments (Abu-Alsoud et al., 2020; Liang et al., 2018a), showing that more hydrophobic compounds were prone to adsorption by MIPs.

4.1.2. Prediction of MIP adsorption properties for volatile phenols: A comparison of empirical data and equilibrium isotherms

The fitness of the adsorption data to various adsorption models is summarized in Table 3. Through comparison of correlation coefficients (R^2), it appears that Langmuir, Freundlich and Halsey fit empirical data for all three volatile phenols well.

The agreements of guaiacol and *m*-cresol with Langmuir (Fig. S1) might on first glance suggest that the binding sites on the surface of the MIPs are homogeneous with adsorption capacity, estimated as 1.235 and 1.684 μmol/g for guaiacol and *m*-cresol, respectively (Table 3), showing that MIPs had a higher adsorption affinity (measured as $\boldsymbol{b}$) for *m*-cresol than guaiacol. However, Scatchard plots (Q_e/C_e Vs C_e in Fig. S6) for guaiacol and *m*-cresol disagreed with the homogeneity (Umpleby II et al., 2004) due to non-linear regressions. Further, given Temkin is based on an assumption that uniform binding energy is distributed on the surface of adsorbents (Johnson & Arnold, 1995; Saadi et al., 2015; Víctor-Ortega et al., 2016), the deviation of Temkin with guaiacol (R^2 = 0.8516) and *m*-cresol (R^2 = 0.7940) might disagree with the homogeneity in the distribution of binding energies on the surface of the MIPs, despite average sorption energies being calculated as 0.0836 and 0.1354 J/kg for guaiacol and *m*-cresol respectively. The exponential slope for Temkin distribution (Fig. S4) might instead indicate the distribution of heat of sorption was exponentially heterogeneous. It is worth noting that Foo and Hameed (2010) reported that Temkin is better suited for modeling gas adsorption equilibrium rather than liquid interactions, which might also be the case in the current study. Additionally, as discussed in the theory section, D-R assumes binding energy is distributed on the heterogeneous surface of adsorbent beads which follows Gaussian energy distribution. Therefore, the fitness of guaiacol, phenol, and *m*-cresol with D-R (Fig. S5) confirms to some extent that the surface of MIPs is heterogeneous with many cavities, which is confirmed by $\boldsymbol{K_{D-R}} < 1$ (López et al., 2012). Furthermore, the adsorption of guaiacol, phenol, and *m*-cresol onto the surface of MIPs can be proposed as chemical sorption because $\boldsymbol{E_{D-R}} > 40$ kJ/mol. The adsorption of other adsorbates (e.g., resveratrol, 3-isobutyl-2-methoxypyrazine, catechin) by MIPs was similarly deemed to be chemical adsorption due to high $\boldsymbol{E_{D-R}}$ (Chen et al., 2013; Liang et al., 2018b; López et al., 2012).

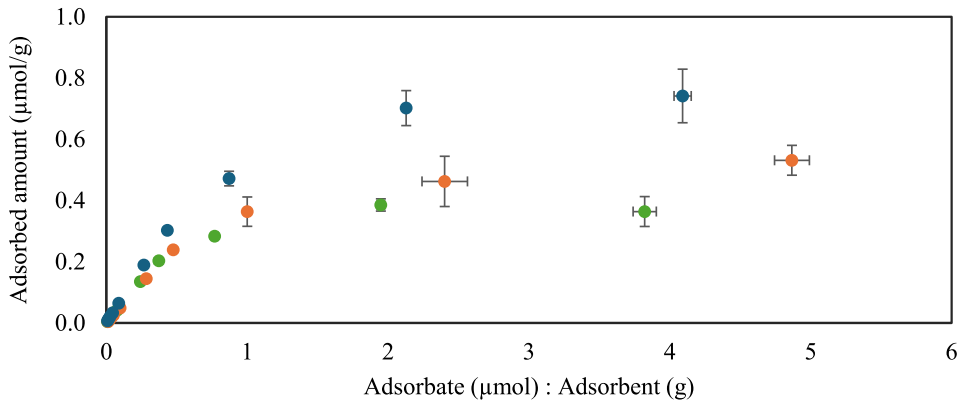

Fig. 2. Effects of adsorbate to adsorbent ratio on uptake of guaiacol (green), phenol (orange), and *m*-cresol (blue) by MIPs. Values are the mean of experimental triplicates with error bars of standard deviation.

Table 3
Isotherm constants calculated for Langmuir, Freundlich, D-R, Temkin and Halsey models.

		Guaiacol	Phenol	*m*-Cresol
Langmuir	Q_{m-L} (μmol/g)	1.235	−0.123	1.684
	b (L/μmol)	9.71 × 10^{-2}	− 5.21 × 10^{-1}	2.083 × 10^{-1}
	R^2	0.9838	0.9687	0.9893
Freundlich	K_F [(μmol/g) (L/μmol)^{n_F}]	0.1163	0.0984	0.2420
	n_F	0.9878	1.1068	0.9189
	R^2	0.9958	0.9959	0.9993
D-R	Q_{m-DR} (μmol/g):	0.203	0.255	0.328
	E_{DR} (kJ/mol):	2689.96	2171.86	3220.78
	K_{DR} (kJ^2/mol^2):	6.91 × 10^{-8}	1.06 × 10^{-7}	4.82 × 10^{-8}
	R^2	0.8724	0.8863	0.8498
Temkin	E_T (J/kg):	0.0836	0.1163	0.1354
	K_T (L/kmol):	11.352	6.7338	18.477
	R^2	0.8516	0.8209	0.7940
Halsey	K_H[(μmol/g) (L/μmol)^{n_H}]:	0.1132	0.1231	0.2135
	n_H	1.0124	0.9035	1.0883
	R^2	0.9958	0.9959	0.9993

Freundlich fits the empirical results for guaiacol and *m*-cresol well (Table 3 and Fig. S2), indicating MIP binding sites were heterogeneous and that there may have been multilayer adsorption. The pre-exponential constant K_F, associated with adsorption capacity and average affinity of the sorbent, was determined to be 0.1163 and 0.2420 for guaiacol and *m*-cresol, respectively; again, MIP adsorption capacity and affinity was higher for *m*-cresol. n_F represents the heterogeneity index, thus a system with a n_F value closer to 1 is considered to be more homogeneous. The comparison of n_F highlighted that in this study, the binding sites occupied by guaiacol (n_F = 0.9878) were more uniform and homogeneous than those occupied by *m*-cresol (n_F = 0.9189).

In contrast, results for phenol (Table 3) showed an inferior adsorption capacity (binding affinity), Q_{m-L} = −0.123 μmol/g for Langmuir and unfavourable adsorption for Freundlich with a higher n_f = 1.1068 > 1, which was also observed in previous studies (Kecili & Hussain, 2018; Liang et al., 2018b; Liu & Wang, 2013; López et al., 2012). The adsorption capacity determined by D-R, being 0.255 μmol/g with a high sorption heat (E_{DR} = 2171.86 kJ/mol) indicated chemisorption of phenol, while the average binding energy determined by Temkin was E_T = 0.1163 J/kg.

These results are consistent with previous adsorption studies using MIPs and other adsorbent products, e.g., the adsorption of 3-isobutyl-2-methoxypyrazine (Liang et al., 2018b), 4-ethylphenol and 4-ethylguaiacol (Filipe-Ribeiro et al., 2020), and resveratrol (Chen et al., 2013) by MIPs in wines, as well as the removal of phenol (Víctor-Ortega et al., 2016), and dyes (Luo et al., 2011; Söylemez et al., 2021) by adsorbent resin in water; all of which gave experimental data that fit multiple isotherm models. Those studies indicated that, when the concentration levels are low, both Langmuir and Freundlich tend to approach linearity and lose some sensitivity in distinguishing homogeneity from heterogeneity (García-Calzón & Díaz-García, 2007; Liang et al., 2018b). Due to the failure of D-R to follow Henry's law at low concentrations (Altın et al., 1998), some uncertainty in the agreement between models and empirical data remained. Additionally, the binding capacity (Q_m) of the systems that follow the Freundlich model are hard to obtain.

Thus, the affinity distribution (AD) of the Freundlich (FIAD) was further analysed using eq. 1 (developed by Umpleby II and co-workers) to measure the continuous distribution of binding affinity on the surface of the MIPs (Umpleby II et al., 2000; 2001; 2004), where: $N(K)$ μg/g represents the number of binding sites as a function of binding affinity (K) L/g.

$$N(K) = 2.303K_F\left(1-{n_F}^2\right)e^{-2.303n_F logK} \quad (1)$$

The apparent number of sites ($N_{K_1-K_2}$) and weighted average affinity ($\overline{K}_{K_1-K_2}$) derived from eq. 1 can be calculated using eqs. 2 and 3 and are presented in Table 4 (Rampey et al., 2004; Umpleby II et al., 2004).

$$N_{K_1-K_2} = K_F\left(1-{n_F}^2\right)\left({K_1}^{-n_F}-{K_2}^{-n_F}\right) \quad (2)$$

$$\overline{K}_{K_1-K_2} = \left(\frac{n_F}{n_F-1}\right)\left[\frac{{K_1}^{1-n_F}-{K_2}^{1-n_F}}{{K_1}^{-n_F}-{K_2}^{-n_F}}\right] \quad (3)$$

$$K_{max} = \frac{1}{C_{emin}} \text{ and } K_{min} = \frac{1}{C_{emax}} \quad (4)$$

The number of apparent binding sites ($N(K)$) calculated for guaiacol and *m*-cresol, within the K limits calculated by eq. 4 (K_{min} and K_{max}), were 0.00988 and 0.1173 μmol/g, with average affinities of 1.3009 and 1.7498 L/μmol towards each phenol (Table 4). This result is consistent with the higher affinity $\overline{K}_{K_1-K_2}$ observed with more hydrophobic compounds (i.e., *m*-cresol vs guaiacol) in Langmuir analysis (Table 3). It is worth mentioning that the estimated $N_{K_1-K_2}$ and $\overline{K}_{K_1-K_2}$ by FIAD can only be trusted within the experimental concentration range. AD also describes the concentration-dependence property of adsorption. Thus, broadening the solute concentration window could increase the affinity distribution and make the description more comprehensive (Umpleby II et al., 2004). The binding sites represented by the area between guaiacol and *m*-cresol in Figure 3 might indicate higher affinity for *m*-cresol than guaiacol.

Halsey was originally developed to describe multilayer adsorption at a relatively large distance from the heterogeneous surface (Liu & Wang, 2013). The agreement of guaiacol and *m*-cresol within this model confirms the nature of the heterogeneity of MIP pores (Table 3 and Fig. S3). Because Halsey is mathematically equivalent to Freundlich (Chu et al.,

Table 4
FIAD parameters over the full concentration range.

Analyte	K_F ($(\mu mol/g)(L/\mu mol)^{n_F}$))	n_F	K limits (L/μmol)	$N_{K_1-K_2}$ (μmol/g)	$\overline{K}_{K_1-K_2}$ (L/μmol)
Guaiacol	0.1163	0.9878	0.2778–26.532	0.00988	1.3009
m-Cresol	0.2420	0.9189	0.2878–55.525	0.1173	1.7498

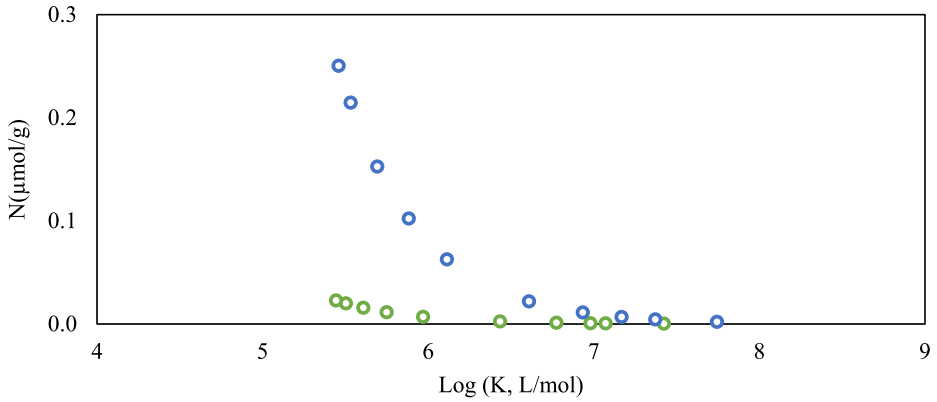

Fig. 3. Affinity distribution of MIP binding sites for guaiacol (green) and *m*-cresol (blue) removal. Values are mean of experimental triplicates.

2023), exactly the same fittings were found for each compound using the two eqs. A similar observation was reported in a study into the adsorption of heavy metal ions by silica-based hybrid adsorbents (Liu & Wang, 2013).

The hybrid Langmuir-Freundlich model developed in 1948 (Sips, 1948), has been previously applied in MIP studies (Abu-Alsoud et al., 2020; Umpleby II et al., 2004), because of its ability to describe saturation behavior at high concentration and to reduce the classic Freundlich at low analyte concentration. However, it was suggested that this hybrid model is not beneficial when the regressions between $logQ_e$ and $logC_e$ are linear (Umpleby II et al., 2004). Consequently, it was not used to characterise MIPs in this study, due to strong linear fit for both guaiacol and *m*-cresol being over the concentration ranges examined (Fig. S2).

The reason behind the low fitting of phenol in models presented in Table 3 remains unclear. Relatively low loading of phenol in model wine could provide an explanation, given that Freundlich and Langmuir approach linearity at a low sorbent concentration (Liang et al., 2018b). The absence of a non-imprinted polymer in the present study makes identification of imprinted sites based on calculation of the imprinting factor (IF) (Ansell, 2015) unachievable.

It is widely recognised that homogeneity is the aim of MIP manufacture, because it underpins the selectivity of the product. However, heterogeneity is inevitable in MIP production (Liang et al., 2018a; Umpleby II et al., 2004); although some imprinting technologies, such as covalent imprinting technology, might lead to higher homogeneity in the affinity distribution of binding sites (Hashim et al., 2014; Rampey et al., 2004; Umpleby II et al., 2000). High-affinity sites in MIPs are prone to rapid occupation whereas low-affinity sites will only be occupied at higher solute concentrations, which characterises MIP behavior as highly concentration-dependent. For that reason, the adsorption character of MIPs determined by fitting empirical results in isotherm equations is more accurate within the experimental concentration range (Rampey et al., 2004). Additionally, inclusion of a broader adsorbate concentration range (i.e., mmol/L vs μmol/L) might result in different adsorbent characterisation results, and is widely used for investigating the adsorption of adsorbates by MIPs in a model wine environment (Du et al., 2023; Filipe-Ribeiro et al., 2020). It should also be noted that capacities and affinities of adsorbents in adsorption studies are usually overestimated compared to practice, due to the minimal binding competition with untargeted compounds (e.g., colour pigments and other volatile compounds in real wines) (Liang et al., 2018a; Liang et al., 2018b). Some additional characterisation studies, e.g., exploring chromatographic separation factors, retention factors or a kinetic study (pseudo-first and second models) might be useful in understanding the adsorption properties of the MIPs (Ansell, 2015; García-Calzón & Díaz-García, 2007).

4.2. Adsorption of volatile phenols by MIPs in smoke tainted wine

4.2.1. Influence of MIP treatment on wine composition

The ultimate goal of the MIP adsorption study was to guide their use in commercial winemaking. Working towards this goal, MIP beads packed in stainless steel columns were used to treat smoke tainted Chardonnay, Cabernet Sauvignon, and rosé wines. Given the greater abundance of colour and phenolic compounds in Cabernet Sauvignon wine (relative to Chardonnay wine), as potential competitors to smoke taint compounds for binding, a higher MIP dose (and lower flow rates) were used to treat Cabernet Sauvignon and rosé wines than the Chardonnay wine (Table 2).

Volatile phenol concentrations in wines before and after treatment are presented in Fig. 4 and Table S2. Significant quantities of volatile phenols were removed following the initial MIP treatment, being 9–37 % for Chardonnay, 10–28 % for Cabernet Sauvignon and 10–29 % for rosé. Further volatile phenol removal was achieved following a second MIP treatment of Chardonnay and Cabernet Sauvignon wines (Fig. 4 and Table S2). However, MIPs were seemingly less efficient at adsorbing syringol from smoke tainted wines; syringol only decreased (by 12 %) following treatment of Cabernet Sauvignon wine (Fig. 4). As such, syringol was not included in the following discussion.

Chardonnay was the first wine treated, and was therefore eluted through a column packed with fresh MIPs. The removal of guaiacol (18 %), *m*-cresol (23 %), *o*-cresol (25 %), phenol (22 %) and 4-methylsyringol (22 %) achieved in Chardonnay after one MIP treatment was significant, relative to untreated Chardonnay. Though additional volatile phenols were adsorbed by the MIPs during the second treatment, the observed decreases were not statistically significant. It was suspected that the column regeneration (involving elution of 2 BVs of 15 % aqueous ethanol) performed between the two Chardonnay treatments did not adequately regenerate the MIPs; as confirmed in the subsequent

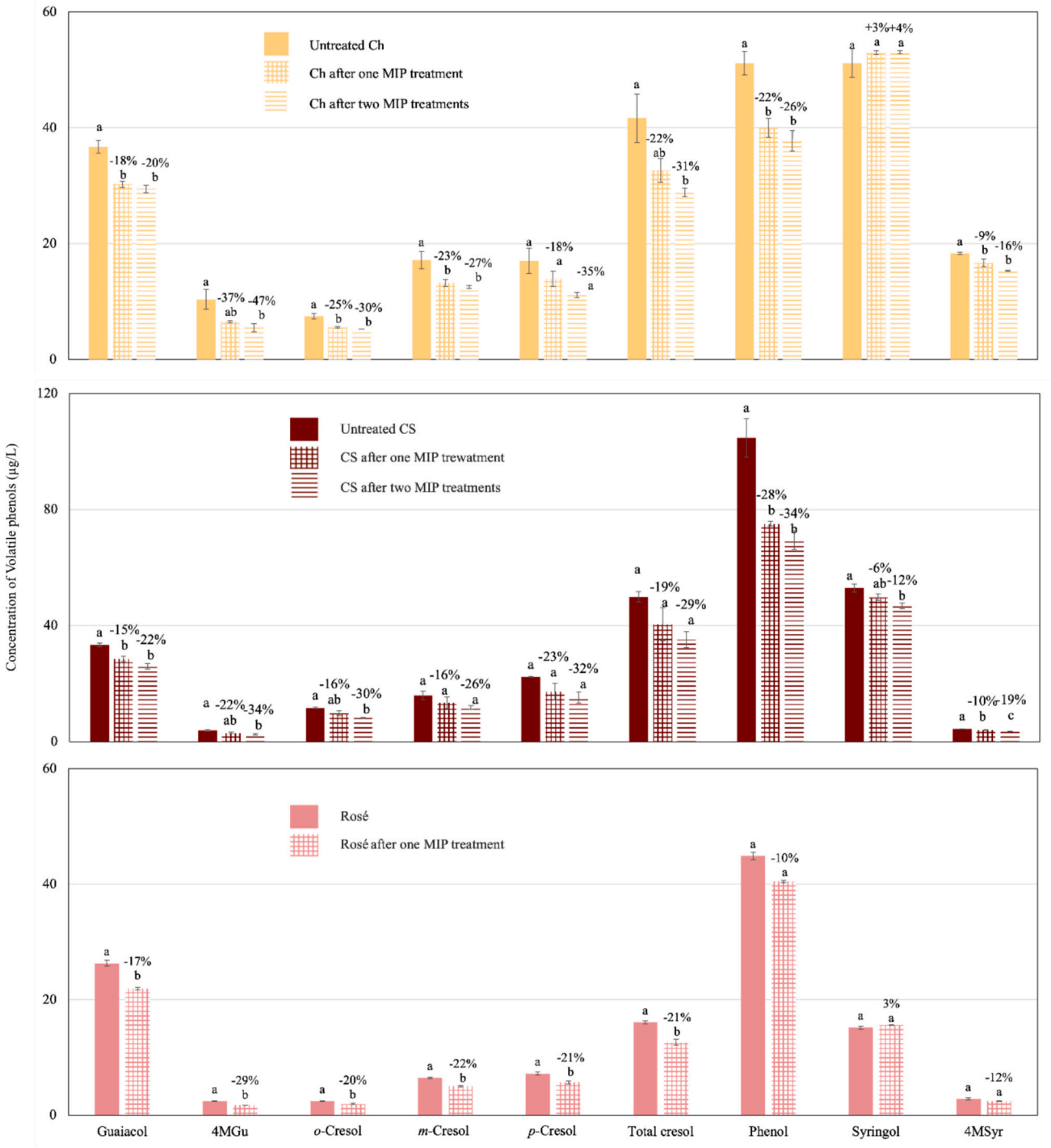

Fig. 4. Concentration (μg/L) of and percentage change in volatile phenols before and after MIP treatment of Chardonnay (Ch), Cabernet Sauvignon (CS) and rosé wines. Values are means of two replicates ± standard deviation. Different letters indicate statistical significance ($p \leq 0.05$, one-way ANOVA) amongst volatile phenol concentrations. 4MGu = 4-methylguaiacol; 4MSyr = 4-methylsyringol.

breakthrough study.

Cabernet Sauvignon (CS) was the second wine to be treated, and it was eluted through the MIP column after a more thorough regeneration (involving elution of 96 % ethanol) than was used between Chardonnay treatments. Again, significant removal of volatile phenols (between 10 and 28 %) was observed following the first MIP treatment of Cabernet Sauvignon, with some volatile phenols also being removed during the second MIP treatment.

The rosé wine was only eluted through the MIP column once (again, after thorough MIP regeneration) resulting in the least removal of volatile phenols, being 17 % for guaiacol, 29 % for 4-methylguaiacol, 22 % for *m*-cresol, 20 % for *o*-cresol, 21 % for *p*-cresol, 10 % for phenol and 12 % for 4-methylsyringol (Fig. 4 and Table S2).

The amount of volatile phenols (μmol) adsorbed per mass of MIPs used (100 g) for each wine treatment is presented in Table S2. As expected, the adsorbed amounts of volatile phenols achieved by MIPs from actual wines during continuous treatment were lower than that estimated in the adsorption isotherm study (i.e., 1.235 and 1.684 μmol/g for guaiacol and *m*-cresol, respectively). This was attributed to MIP concentration-dependent adsorption capacity towards different volatile

phenols due to their heterogeneity, as well as binding competition from other phenolic compounds in wine.

Furthermore, no significant removal of volatile phenol glycoconjugates was evident comparing the composition of treated wines to their corresponding controls (Table S3), in agreement with previous fermentation studies (Huo et al., 2024).

The sorption of wine colour and phenolic compounds by the column packed MIPs is presented in Table S4. Statistically significant decreases were observed with total phenolics and brown pigments measurements for MIP-treated Chardonnay wines, however, this accounted for only 6–9 % losses relative to untreated wine.

No detrimental effects of MIP treatment on the wine colour density or phenolic composition were apparent for Cabernet Sauvignon or rosé wines (Table S4). Wine colour density for Cabernet Sauvignon was slightly lower (by 3–6 %) which likely reflected decreased SO_2 pigments (2–6 %). However, the concentration of anthocyanins, total phenolics, and red pigments increased by 3–6 %, >6 %, and > 4 %, respectively, with greater differences observed in wines after the first MIP treatment than the second. In contrast, MIP treated rosé wine had higher hue (17 %), SO_2-resistant pigments (5 %) and total red pigments (11 %), but had lower wine colour density (6 %) and total phenolics, compared with untreated rosé.

The limited removal of volatile phenol glycoconjugates and colour-related compounds observed during treatment of the three smoke tainted wines demonstrates the greater adsorption affinities of MIP towards volatile phenols, as intended. This finding was similar to observations reported by Filipe-Ribeiro et al. (2020) in a study that used MIPs imprinted with 4-ethylphenol (4-EP) and 4-ethylguaiacol (4-EG) to remove volatile phenols from wine; 38–63 % of 4-EP and 4-EG were removed, but with limited impact on colour density (which decreased by only 14 %).

4.2.2. Impact of MIP treatment on wine sensory profiles

The sensory profiles of untreated and treated wines are presented in Table S5. The sensory panel perceived the treated Cabernet Sauvignon to be significantly less smoky compared with its corresponding untreated wine, with less intense cold ash, earthy and medicinal aromas, smoky flavor and woody aftertaste. Overall fruit aroma and flavor increased with treatment, likely reflecting the unmasking of fruit characters following removal of volatile phenols (Huo et al., 2024; Ristic et al., 2016). In contrast, fruit expression decreased in treated Chardonnay and rosé wines (Table S5), which suggests some removal of fruit-related volatile compounds by the MIPs, as reported previously (Huo et al., 2024). Aromas associated with oxidation were also evident in treated Chardonnay and rosé wines, possibly due to exposure to air retained in the porous MIP beads and/or the column during treatment of wine which in turn could potentially be mitigated in future by pre-flushing the column and lines with nitrogen prior to wine treatment.

4.3. MIP breakthrough study

4.3.1. Breakthrough of volatile phenols

A breakthrough study was conducted to evaluate MIP saturation, by comparing the concentration of volatile phenols present in effluent and influent. It is generally recognised that column breakthrough occurs when the concentration ratio between the inlet and the outlet reaches 0.05 (i.e. 5 % of the initial concentration of a target compound can be detected in the effluent), while saturation occurs when the ratio reaches 0.9, i.e. 90 % of the initial concentration of a target compound can be detected in the effluent (Ateia et al., 2020; Chowdhury et al., 2015). Column effluent concentrations were monitored at regular intervals during treatments of each smoke tainted wine to determine the MIP breakthrough point for each volatile phenol.

According to the results presented in Figs. 5 and S7, MIPs did not remove syringol from any of the smoke tainted wines during treatment. Consistently high outlet-to-inlet ratios (i.e., > 0.9) were observed for syringol, while the effluent levels of other volatile phenols increased as a function of the volume of wine treated. The lowest passage (greatest removal) of volatile phenols was observed in the first effluent fraction collected for each wine (being 38–74 % for Chardonnay, 47–80 % for Cabernet Sauvignon, and 43–73 % for rosé). Amongst the volatile phenols, the lowest removal was observed for 4-methylsyringol, for all wines, indicating MIPs may have higher affinity towards guaiacol, cresols, phenol, and 4-methylguaiacol over syringol and 4-methylsyringol.

The delayed breakthrough curves in all three wines confirmed satisfactory regeneration of MIPs after each wine treatment. However, the actual breakpoint (ratio = 0.05 (Chowdhury et al., 2015)) for each volatile phenol could not be identified as it might happen at any point during the treatment of the first batch of wines (10 BVs of Chardonnay and 7 BVs of Cabernet Sauvignon and rosé).

During the first MIP treatment of Chardonnay (Fig. 5), MIPs were saturated (ratio = 0.9) by different volatile phenols at different stages, e.g., 4-methylsyringol saturation occurred first (at 40 BVs), then guaiacol (50 BVs), phenol (60 BVs), *p*-cresol (70 BVs), *o*- and *m*-cresol (80 BVs), and 4-methylguaiacol (beyond 80 BVs). From the point of MIP saturation (ratio > 0.9), the outlet/inlet ratios remained constant throughout subsequent elution of Chardonnay wine, including during the second MIP treatment. The plateau of breakthrough curves suggested that the rapid regeneration (eluting the MIP column with 2 BVs of 15 % aqueous ethanol) applied between the two Chardonnay treatments did not release a meaningful proportion of binding sites to enable any subsequent remediation (i.e., regeneration was not achieved).

A similar trend was observed for Cabernet Sauvignon treatment in terms of the removal of volatile phenols (Fig. S7). The concentration ratios of volatile phenols were initially between 0.47 and 0.8, but saturation was reached after elution of approximately 28 BVs of wine, which was earlier than for Chardonnay. The concentration ratios decreased from 1.0 to between 0.56 and 0.74 for the first effluent fraction collected during the second MIP treatment of Cabernet Sauvignon wine. This confirmed improved regeneration of the MIPs (using 96 % ethanol) than occurred between Chardonnay treatments.

The rosé wine was only treated a single time, and concentration ratios were again between 0.41 and 0.73 initially, but saturated at ~28 BVs (Fig. S7).

4.3.2. Breakthrough of wine colour and volatile phenol glycoconjugates

The colour and volatile phenol glycoconjugate content of column effluent generated during MIP treatment of smoke tainted Chardonnay, Cabernet Sauvignon and rosé wines are presented in Tables S6, S7 and S8, respectively.

As discussed in the previous section, the impact of MIP treatment on wine colour was limited. Changes in A280 and A420 absorbance in effluent collected during sequential Chardonnay treatments were < 6–7 % and 7–9 %, respectively (Table S4). Similar changes were observed during treatment of Cabernet Sauvignon and rosé wines (Table S4).

Column break through (i.e., concentration ratio for outlet/inlet = 0.9) by volatile phenol glycoconjugates occurred instantly, for all wine treatments. Though some removal of volatile phenol glycosides was noted for the first sampling of treated Chardonnay and Cabernet Sauvignon wines, changes in concentration were not statistically significant (Tables S3, S7 and S8). Decreases in guaiacol and 4-methylguaiacol glycosides were observed in treated rosé wine at the first sampling point, but overall changes in concentration for treated rosé wine were not significant (Table S3 and S8).

4.4. Reusability of MIPs

Throughout the semi-commercial remediation trial, the same batch of MIP beads (~700–1000 g/replicate) were used to treat 480 L of wine (160 L each of Chardonnay, Cabernet Sauvignon and rosé), with thorough regeneration (with 96 % ethanol) following treatment of Chardonnay wine, and each Cabernet Sauvignon treatments. Because the

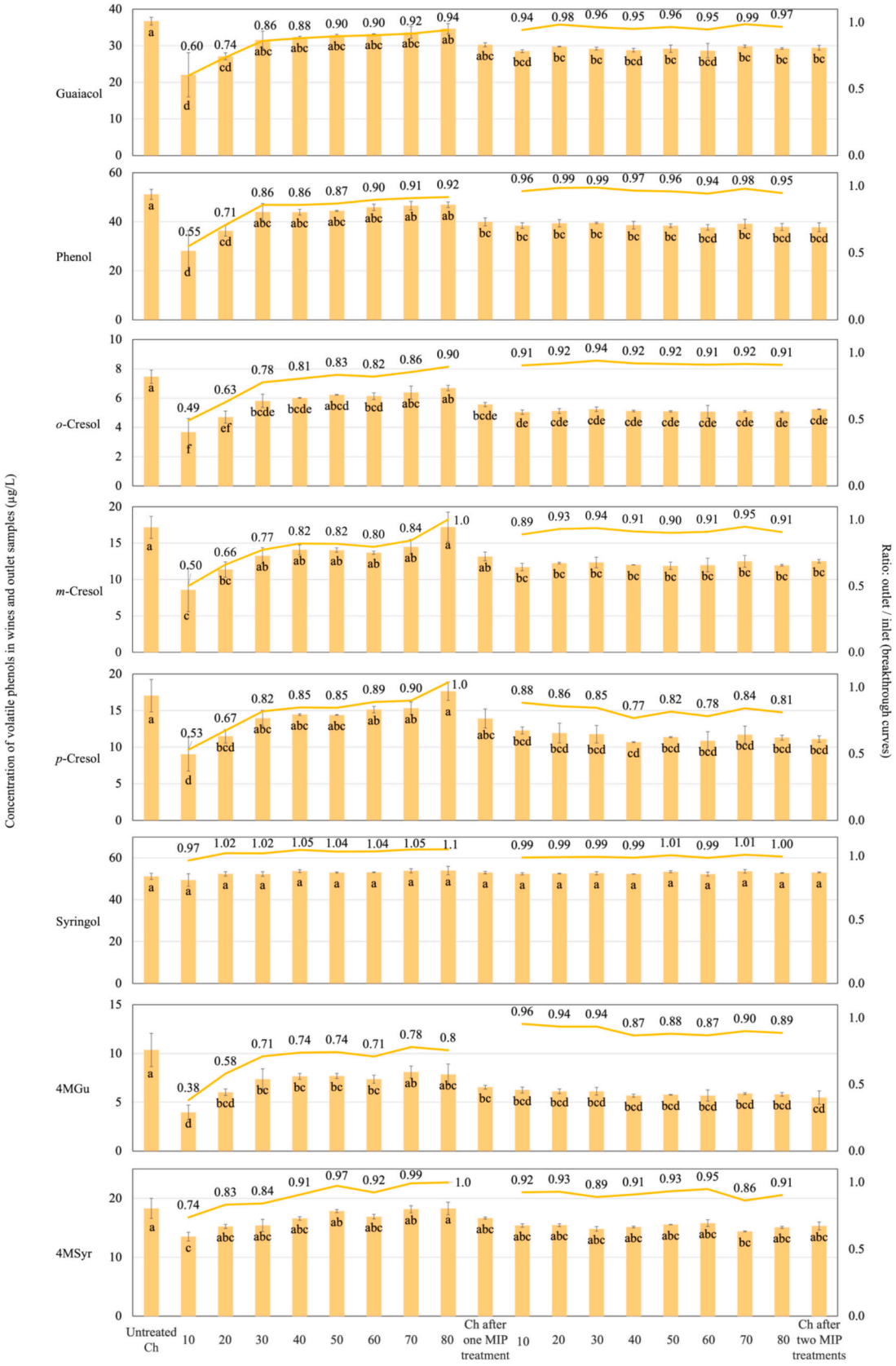

Fig. 5. Changes in influent and effluent concentrations of volatile phenols (and their concentration ratios; i.e., outlet/inlet breakthrough curves,) during treatment of Chardonnay (Ch) wine via elution through a fixed-bed-column packed with MIPs. Values are means of two replicates ± standard deviation. Different letters indicate statistical significance ($p \leq 0.05$, one-way ANOVA) amongst volatile phenol concentrations. 4MGu = 4-methylguaiacol, 4MSyr = 4-methylsyringol.

outlet/inlet ratios of volatile phenols were ranging from 0.38 to 0.74 (excluding syringol) after each regeneration, it is clear that MIPs can be successfully reused multiple times.

5. Conclusions

The potential of a commercial MIP to adsorb volatile phenols in a model wine environment (i.e., without competition from other wine constituents) was demonstrated via an adsorption study, with the adsorption capacity for guaiacol and *m*-cresol estimated to be 1.235 and 1.684 μmol/g, respectively. Multiple adsorption models confirmed the MIPs had a higher adsorption affinity towards *m*-cresol than guaiacol. Alignment of experimental data to Freundlich and D-R adsorption models demonstrated heterogeneity of MIPs, which is not unexpected given that heterogeneity is inevitable in MIP production. When column-packed MIPs were used to treat smoke tainted wines, 16 to 47 %, 19 to 34 % and 12 to 29 % removal of smoke-derived volatile phenols (excluding syringol) was achieved depending on wine style treated; importantly with only small concomitant losses in wine colour. Sensory analysis confirmed smoke-related attributes were significantly diminished (and fruit expression enhanced) following treatment of Cabernet Sauvignon wine, but the sensory outcomes for Chardonnay and rosé wines were less obvious. Volatile phenol glycosides were not meaningfully removed.

Studies of the binding capacity of the MIP column established that saturation with volatile phenols occurred after elution of 40 to 80 BVs of smoke tainted Chardonnay wine and after 28 BVs of smoke tainted Cabernet Sauvignon and rosé wines. Further research is warranted for optimising column operating conditions, to delay saturation, as well as MIP regeneration and minimising the reliance on concentrated ethanol, in order to facilitate the use of MIPs for commercial winemaking applications.

Funding

This research was funded by the Australian Government as part of a Cooperative Research Centre Project (project number CRCPIX000220), with financial and in-kind support from industry partners: Cassegrain Wines, amaea, the Australian Wine Research Institute, VAF Memstar, and De Beaurepaire Wines). Y.H. was the recipient of a Wine Australia supplementary scholarship (project number WAPh2003).

CRediT authorship contribution statement

Yiming Huo: Writing – review & editing, Writing – original draft, Visualization, Validation, Methodology, Investigation, Formal analysis, Data curation, Conceptualization. **Renata Ristic:** Writing – review & editing, Methodology, Investigation, Formal analysis. **Maxime Savoie:** Writing – review & editing, Resources, Methodology, Conceptualization. **Richard Muhlack:** Writing – review & editing, Validation, Supervision, Methodology, Formal analysis, Conceptualization. **Markus Herderich:** Writing – review & editing, Supervision, Methodology, Conceptualization. **Kerry Wilkinson:** Writing – review & editing, Validation, Supervision, Resources, Project administration, Methodology, Funding acquisition, Data curation, Conceptualization.

Declaration of competing interest

The authors declare the following financial interests/personal relationships which may be considered as potential competing interests: Kerry Wilkinson reports financial support was provided by Cooperative Research Centres Program. Kerry Wilkinson reports financial support and equipment, drugs, or supplies were provided by Cassegrain Wines. Kerry Wilkinson reports financial support and equipment, drugs, or supplies were provided by amaea. Kerry Wilkinson reports financial support and equipment, drugs, or supplies were provided by The Australian Wine Research Institute Limited. Kerry Wilkinson reports financial support was provided by De Beaurepaire Wines. Yiming Huo reports financial support was provided by Wine Australia. Maxime Savoie reports a relationship with amaea that includes: employment. Markus Herderich reports a relationship with The Australian Wine Research Institute Limited that includes: employment. If there are other authors, they declare that they have no known competing financial interests or personal relationships that could have appeared to influence the work reported in this paper.

Data availability

The data that has been used is confidential.

Acknowledgements

The authors gratefully acknowledge: amaea for the provision of molecularly imprinted polymers and technical support; Assoc. Prof. David Jeffery for advice on the adsorption isotherm study; John and Alex Cassegrain (Cassegrain Wines) for access to the smoke tainted wines, facilities and technical support needed for the remediation trials; and the panelists who participated in sensory analysis.

Appendix A. Supplementary data

Supplementary data to this article can be found online at https://doi.org/10.1016/j.foodres.2025.116048.

References

Abu-Alsoud, G. F., Hawboldt, K. A., & Bottaro, C. S. (2020). Comparison of four adsorption isotherm models for characterizing molecular recognition of individual phenolic compounds in porous tailor-made molecularly imprinted polymer films. *ACS Applied Materials & Interfaces, 12*(10), 11998–12009. https://doi.org/10.1021/acsami.9b21493

Altın, O., Özbelge, H.Ö., & Doğu, T. (1998). Use of general purpose adsorption isotherms for heavy metal–clay mineral interactions. *Journal of Colloid and Interface Science, 198*(1), 130–140. https://doi.org/10.1006/jcis.1997.5246

Ansell, R. J. (2015). Characterization of the binding properties of molecularly imprinted polymers. *Molecularly Imprinted Polymers in Biotechnology*, 51–93.

Ares, G., Bruzzone, F., Vidal, L., Cadena, R. S., Giménez, A., Pineau, B., … Jaeger, S. R. (2014). Evaluation of a rating-based variant of check-all-that-apply questions: Rate-all-that-apply (RATA). *Food Quality and Preference, 36*, 87–95. https://doi.org/10.1016/j.foodqual.2014.03.006

Ateia, M., Helbling, D. E., & Dichtel, W. R. (2020). Best practices for evaluating new materials as adsorbents for water treatment. *ACS Materials Letters, 2*, 1532–1544. https://doi.org/10.1021/acsmaterialslett.0c00414

Ayawei, N., Ebelegi, A. N., & Wankasi, D. (2017). Modelling and interpretation of adsorption isotherms. *Journal of Chemistry, 2017*, 1–11. https://doi.org/10.1155/2017/3039817

BelBruno, J. J. (2019). Molecularly imprinted polymers. *Chemical Reviews, 119*, 94–119. https://doi.org/10.1021/acs.chemrev.8b00171

Bilogrevic, E., Jiang, W., Culbert, J., Francis, L., Herderich, M., & Parker, M. (2023). Consumer response to wine made from smoke-affected grapes. *OENO one, 57*(2), 417–430. https://doi.org/10.20870/oeno-one.2023.57.2.7261

Cengiz, N., Guclu, G., Kelebek, H., Capanoglu, E., & Selli, S. (2022). Application of molecularly imprinted polymers for the detection of volatile and off-odor compounds in food matrices. *ACS Omega, 7*, 15258–15266. https://doi.org/10.1021/acsomega.1c07288

Chatonnet, P., Dubourdie, D., Boidron, J., & n., & Pons, M.. (1992). The origin of ethylphenols in wines. *Journal of the Science of Food and Agriculture, 60*(2), 165–178. https://doi.org/10.1002/jsfa.2740600205

Chen, F.-F., Xie, X.-Y., & Shi, Y.-P. (2013). Preparation of magnetic molecularly imprinted polymer for selective recognition of resveratrol in wine. *Journal of Chromatography A, 1300*, 112–118. https://doi.org/10.1016/j.chroma.2013.02.018

Chowdhury, Z. Z., Abd Hamid, S. B., & Zain, S. M. (2015). Evaluating design parameters for breakthrough curve analysis and kinetics of fixed bed columns for cu (II) cations using lignocellulosic wastes. *BioResources, 10*(1), 732–749.

Chu, K. H., Bashiri, H., Hashim, M. A., Abd Shukor, M. Y., & Bollinger, J.-C. (2023). The Halsey isotherm for water contaminant adsorption is fake. *Separation and Purification Technology, 313*, Article 123500. https://doi.org/10.1016/j.seppur.2023.123500

Crump, A. M., Sefton, M. A., & Wilkinson, K. L. (2014). Microwave-assisted deuterium exchange: The convenient preparation of isotopically labelled analogues for stable isotope dilution analysis of volatile wine phenols. *Food Chemistry, 162*, 261–263. https://doi.org/10.1016/j.foodchem.2014.04.051

Culbert, J. A., Jiang, W., Bilogrevic, E., Likos, D., Francis, I. L., Krstic, M. P., & Herderich, M. J. (2021). Compositional changes in smoke-affected grape juice as a

consequence of activated carbon treatment and the impact on phenolic compounds and smoke flavor in wine. *Journal of Agricultural and Food Chemistry, 69*(35), 10246–10259. https://doi.org/10.1021/acs.jafc.1c02642

Dang, C., Jiranek, V., Taylor, D. K., & Wilkinson, K. L. (2020). Removal of volatile phenols from wine using crosslinked cyclodextrin polymers. *Molecules, 25*(4), 910. https://doi.org/10.3390/molecules25040910

Du, G., Wang, X., & Zhao, Q. (2023). Targeted removal of galloylated flavanols to adjust wine astringency by using molecular imprinting technology. *Foods, 12*(18), 3331. https://doi.org/10.3390/foods12183331

Dungey, K. A., Hayasaka, Y., & Wilkinson, K. L. (2011). Quantitative analysis of glycoconjugate precursors of guaiacol in smoke-affected grapes using liquid chromatography–tandem mass spectrometry based stable isotope dilution analysis. *Food Chemistry, 126*, 801–806. https://doi.org/10.1016/j.foodchem.2010.11.094

Estreicher, S. K. (2017). The beginning of wine and viticulture. *Physica Status Solidi C, 14*(7), 1700008. https://doi.org/10.1002/pssc.201700008

Favell, J. W., Fordwour, O. B., Morgan, S. C., Zigg, I., & Zandberg, W. F. (2021). Large-scale reassessment of in-vineyard smoke-taint grapevine protection strategies and the development of predictive off-vine models. *Molecules, 26*, 4311. https://doi.org/10.3390/molecules26144311

Favell, J. W., Noestheden, M., Lyons, S. M., & Zandberg, W. F. (2019). Development and evaluation of a vineyard-based strategy to mitigate smoke-taint in wine grapes. *Journal of Agricultural and Food Chemistry, 67*, 14137–14142. https://doi.org/10.1021/acs.jafc.9b05859

Filipe-Ribeiro, L., Cosme, F., & Nunes, F. M. (2020). New molecularly imprinted polymers for reducing negative volatile phenols in red wine with low impact on wine colour. *Food Research International, 129*, Article 108855. https://doi.org/10.1016/j.foodres.2019.108855

Foo, K. Y., & Hameed, B. H. (2010). Insights into the modeling of adsorption isotherm systems. *Chemical Engineering Journal, 156*(1), 2–10. https://doi.org/10.1016/j.cej.2009.09.013

Freundlich, H. (1906). Over the adsorption in solution. *Journal of Physical Chemistry, 57*(385471), 1100–1107.

Fudge, A. L., Ristic, R., Wollan, D., & Wilkinson, K. L. (2011). Amelioration of smoke taint in wine by reverse osmosis and solid phase adsorption. *Australian Journal of Grape and Wine Research, 17*, S41–S48. https://doi.org/10.1111/j.1755-0238.2011.00148.x

Fudge, A. L., Schiettecatte, M., Ristic, R., Hayasaka, Y., & Wilkinson, K. L. (2012). Amelioration of smoke taint in wine by treatment with commercial fining agents. *Australian Journal of Grape and Wine Research, 18*, 302–307. https://doi.org/10.1111/j.1755-0238.2012.00200.x

García-Calzón, J. A., & Díaz-García, M. E. (2007). Characterization of binding sites in molecularly imprinted polymers. *Sensors and Actuators B: Chemical, 123*(2), 1180–1194. https://doi.org/10.1016/j.snb.2006.10.068

Hashim, S. N., Boysen, R. I., Schwarz, L. J., Danylec, B., & Hearn, M. T. (2014). A comparison of covalent and non-covalent imprinting strategies for the synthesis of stigmasterol imprinted polymers. *Journal of Chromatography A, 1359*, 35–43. https://doi.org/10.1016/j.chroma.2014.07.034

Hayasaka, Y., Dungey, K., Baldock, G., Kennison, K., & Wilkinson, K. (2010b). Identification of a β-D-glucopyranoside precursor to guaiacol in grape juice following grapevine exposure to smoke. *Analytica Chimica Acta, 660*, 143–148. https://doi.org/10.1016/j.aca.2009.10.039

Hayasaka, Y., Parker, M., Baldock, G. A., Pardon, K. H., Black, C. A., Jeffery, D. W., & Herderich, M. J. (2013). Assessing the impact of smoke exposure in grapes: Development and validation of a HPLC-MS/MS method for the quantitative analysis of smoke-derived phenolic glycosides in grapes and wine. *Journal of Agricultural and Food Chemistry, 61*, 25–33. https://doi.org/10.1021/jf305025j

Hayasaka, Y., Baldock, G. A., Parker, M., Pardon, K. H., Black, C. A., Herderich, M. J., & Jeffery, D. W. (2010a). Glycosylation of smoke-derived volatile phenols in grapes as a consequence of grapevine exposure to bushfire smoke. *Journal of Agricultural and Food Chemistry, 58*, 10989–10998. https://doi.org/10.1021/jf103045t

Huo, Y., Ristic, R., Puglisi, C., Wang, X., Muhlack, R., Baars, S., … Wilkinson, K. L. (2024). Amelioration of smoke taint in wine via addition of molecularly imprinted polymers during or after fermentation. *Journal of Agricultural and Food Chemistry, 72*(32), 18121–18131. https://doi.org/10.1021/acs.jafc.4c03912

Johnson, R. D., & Arnold, F. H. (1995). The Temkin isotherm describes heterogeneous protein adsorption. *Biochimica et Biophysica Acta (BBA) - Protein Structure and Molecular Enzymology, 1247*(2), 293–297. https://doi.org/10.1016/0167-4838(95)00006-G

Kecili, R., & Hussain, C. M. (2018). Mechanism of adsorption on nanomaterials. In *Nanomaterials in chromatography* (pp. 89–115). Elsevier.

Kennison, K., Wilkinson, K. L., Pollnitz, A., Williams, H., & Gibberd, M. R. (2009). Effect of timing and duration of grapevine exposure to smoke on the composition and sensory properties of wine. *Australian Journal of Grape and Wine Research, 15*, 228–237. https://doi.org/10.1111/j.1755-0238.2009.00056.x

Kennison, K., Wilkinson, K. L., Williams, H. G., Smith, J. H., & Gibberd, M. R. (2007). Smoke-derived taint in wine: Effect of postharvest smoke exposure of grapes on the chemical composition and sensory characteristics of wine. *Journal of Agricultural and Food Chemistry, 55*, 10897–10901. https://doi.org/10.1021/jf072509k

Langmuir, I. (1918). The adsorption of gases on plane surfaces of glass, mica and platinum. *Journal of the American Chemical Society, 40*(9), 1361–1403.

Liang, C., Boss, P. K., & Jeffery, D. W. (2018a). Extraction properties of new polymeric sorbents applied to wine. *Journal of Agricultural and Food Chemistry, 66*, 10086–10096. https://doi.org/10.1021/acs.jafc.8b04641

Liang, C., Jeffery, D. W., & Taylor, D. K. (2018b). Preparation of magnetic polymers for the elimination of 3-isobutyl-2-methoxypyrazine from wine. *Molecules, 23*, 1140. https://doi.org/10.3390/molecules23051140

Liu, J., & Wang, X. (2013). Novel silica-based hybrid adsorbents: Lead (II) adsorption isotherms. *The Scientific World Journal, 2013*. https://doi.org/10.1155/2013/897159

Liu, Y., Zhang, H., Xie, D., Lai, H., Qiu, Q., & Ma, X. (2022). Optimized synthesis of molecularly imprinted polymers coated magnetic UIO-66 MOFs for simultaneous specific removal and determination of multi types of macrolide antibiotics in water. *Journal of Environmental Chemical Engineering, 10*, Article 108094. https://doi.org/10.1016/j.jece.2022.108094

López, M. D. M. C., Pérez, M. C., García, M. S. D., Vilariño, J. M. L., Rodríguez, M. V. G., & Losada, L. F. B. (2012). Preparation, evaluation and characterization of quercetin-molecularly imprinted polymer for preconcentration and clean-up of catechins. *Analytica Chimica Acta, 721*, 68–78. https://doi.org/10.1016/j.aca.2012.01.049

Luo, X., Zhan, Y., Huang, Y., Yang, L., Tu, X., & Luo, S. (2011). Removal of water-soluble acid dyes from water environment using a novel magnetic molecularly imprinted polymer. *Journal of Hazardous Materials, 187*, 274–282. https://doi.org/10.1016/j.jhazmat.2011.01.009

Mercurio, M. D., Dambergs, R. G., Herderich, M. J., & Smith, P. A. (2007). High throughput analysis of red wine and grape phenolics adaptation and validation of methyl cellulose precipitable tannin assay and modified Somers color assay to a rapid 96 well plate format. *Journal of Agricultural and Food Chemistry, 55*, 4651–4657. https://doi.org/10.1021/jf063674n

Murray, A., & Örmeci, B. (2012). Application of molecularly imprinted and non-imprinted polymers for removal of emerging contaminants in water and wastewater treatment: A review. *Environmental Science and Pollution Research, 19*(9), 3820–3830. https://doi.org/10.1007/s11356-012-1119-2

Noestheden, M., Dennis, E. G., Romero-Montalvo, E., DiLabio, G. A., & Zandberg, W. F. (2018). Detailed characterization of glycosylated sensory-active volatile phenols in smoke-exposed grapes and wine. *Food Chemistry, 259*, 147–156. https://doi.org/10.1016/j.foodchem.2018.03.097

Oliveira, C. M., Ferreira, A. C. S., De Freitas, V., & Silva, A. M. (2011). Oxidation mechanisms occurring in wines. *Food Research International, 44*(5), 1115–1126. https://doi.org/10.1016/j.foodres.2011.03.050

Ortega, A., Lopez-Toledano, A., Mayen, M., Merida, J., & Medina, M. (2003). Changes in color and phenolic compounds during oxidative aging of sherry white wine. *Journal of Food Science, 68*(8), 2461–2468. https://doi.org/10.1111/j.1365-2621.2003.tb07046.x

Parker, M., Osidacz, P., Baldock, G. A., Hayasaka, Y., Black, C. A., Pardon, K. H., … Francis, I. L. (2012). Contribution of several volatile phenols and their glycoconjugates to smoke-related sensory properties of red wine. *Journal of Agricultural and Food Chemistry, 60*, 2629–2637. https://doi.org/10.1021/jf2040548

Pereira, C. S., Marques, J. J. F., & San Romão, M. V. (2000). Cork taint in wine: Scientific knowledge and public perception — A critical review. *Critical Reviews in Microbiology, 26*(3), 147–162. https://doi.org/10.1080/10408410008984174

Pickering, G. J., & Botezatu, A. (2021). A review of ladybug taint in wine: Origins, prevention, and remediation. *Molecules, 26*(14), 4341. https://doi.org/10.3390/molecules26144341

Pollnitz, A. P., Pardon, K. H., Sykes, M., & Sefton, M. A. (2004). The effects of sample preparation and gas chromatograph injection techniques on the accuracy of measuring guaiacol, 4-methylguaiacol and other volatile oak compounds in oak extracts by stable isotope dilution analyses. *Journal of Agricultural and Food Chemistry, 52*, 3244–3252. https://doi.org/10.1021/jf035380x

Puglisi, C., Ristic, R., Saint, J., & Wilkinson, K. (2022). Evaluation of spinning cone column distillation as a strategy for remediation of smoke taint in juice and wine. *Molecules, 27*(22), 8096. https://doi.org/10.3390/molecules27228096

Rampey, A. M., Umpleby, R. J., Rushton, G. T., Iseman, J. C., Shah, R. N., & Shimizu, K. D. (2004). Characterization of the imprint effect and the influence of imprinting conditions on affinity, capacity, and heterogeneity in molecularly imprinted polymers using the Freundlich isotherm-affinity distribution analysis. *Analytical Chemistry, 76*(4), 1123–1133. https://doi.org/10.1021/ac0345345

Ristic, R., Boss, P. K., & Wilkinson, K. L. (2015). Influence of fruit maturity at harvest on the intensity of smoke taint in wine. *Molecules, 20*, 8913–8927. https://doi.org/10.3390/molecules20058913

Ristic, R., Fudge, A. L., Pinchbeck, K. A., De Bei, R., Fuentes, S., Hayasaka, Y., … Wilkinson, K. L. (2016). Impact of grapevine exposure to smoke on vine physiology and the composition and sensory properties of wine. *Theoretical and Experimental Plant Physiology, 28*, 67–83. https://doi.org/10.1007/s40626-016-0054-x

Ristic, R., Osidacz, P., Pinchbeck, K., Hayasaka, Y., Fudge, A., & Wilkinson, K. L. (2011). The effect of winemaking techniques on the intensity of smoke taint in wine. *Australian Journal of Grape and Wine Research, 17*, S29–S40. https://doi.org/10.1111/j.1755-0238.2011.00146.x

Saadi, R., Saadi, Z., Fazaeli, R., & Fard, N. E. (2015). Monolayer and multilayer adsorption isotherm models for sorption from aqueous media. *Korean Journal of Chemical Engineering, 32*(5), 787–799. https://doi.org/10.1007/s11814-015-0053-7

Sefton, M. A., & Simpson, R. F. (2005). Compounds causing cork taint and the factors affecting their transfer from natural cork closures to wine – A review. *Australian Journal of Grape and Wine Research, 11*(2), 226–240. https://doi.org/10.1111/j.1755-0238.2005.tb00290.x

Sellergren, B., & Hall, A. J. (2012). Molecularly imprinted polymers. In *Supramolecular Chemistry*. John Wiley & Sons, Ltd.. https://doi.org/10.1002/9780470661345.smc137

Shahnaz, T., Sharma, V., Subbiah, S., & Narayanasamy, S. (2020). Multivariate optimisation of Cr (VI), co (III) and cu (II) adsorption onto nanobentonite incorporated nanocellulose/chitosan aerogel using response surface methodology. *Journal of Water Process Engineering, 36*, Article 101283. https://doi.org/10.1016/j.jwpe.2020.101283

Sims, C. A., Eastridge, J. S., & Bates, R. P. (1995). Changes in phenols, color, and sensory characteristics of muscadine wines by pre-and post-fermentation additions of PVPP, casein, and gelatin. *American Journal of Enology and Viticulture, 46*(2), 155–158. https://doi.org/10.5344/ajev.1995.46.2.155

Sips, R. (1948). On the structure of a catalyst surface. *The Journal of Chemical Physics, 16*(5), 490–495. https://doi.org/10.1063/1.1746922

Söylemez, M. A., Okan, M., Güven, O., & Barsbay, M. (2021). Synthesis of well-defined molecularly imprinted bulk polymers for the removal of azo dyes from water resources. *Current Research in Green and Sustainable Chemistry, 4*, Article 100196. https://doi.org/10.1016/j.crgsc.2021.100196

Szeto, C., Ristic, R., & Wilkinson, K. (2022). Thinking inside the box: A novel approach to smoke taint mitigation trials. *Molecules, 27*, 1667. https://doi.org/10.3390/molecules27051667

Umpleby, R. J., II, Baxter, S. C., Bode, M., Berch, J. K., Jr., Shah, R. N., & Shimizu, K. D. (2001). Application of the Freundlich adsorption isotherm in the characterization of molecularly imprinted polymers. *Analytica Chimica Acta, 435*(1), 35–42. https://doi.org/10.1016/S0003-2670(00)01211-3

Umpleby, R. J., II, Baxter, S. C., Rampey, A. M., Rushton, G. T., Chen, Y., & Shimizu, K. D. (2004). Characterization of the heterogeneous binding site affinity distributions in molecularly imprinted polymers. *Journal of Chromatography B, 804*(1), 141–149. https://doi.org/10.1016/j.jchromb.2004.01.064

Umpleby, R. J., II, Bode, M., & Shimizu, K. D. (2000). Measurement of the continuous distribution of binding sites in molecularly imprinted polymers. *Analyst, 125*(7), 1261–1265. https://doi.org/10.1039/b002354j

Vasapollo, G., Sole, R. D., Mergola, L., Lazzoi, M. R., Scardino, A., Scorrano, S., & Mele, G. (2011). Molecularly imprinted polymers: Present and future prospective. *International Journal of Molecular Sciences, 12*, 5908–5945. https://doi.org/10.3390/ijms12095908

Víctor-Ortega, M., Ochando-Pulido, J., & Martínez-Férez, A. (2016). Phenols removal from industrial effluents through novel polymeric resins: Kinetics and equilibrium studies. *Separation and Purification Technology, 160*, 136–144. https://doi.org/10.1016/j.seppur.2016.01.023

Waters, E. J., Alexander, G., Muhlack, R., Pocock, K., Colby, C., & O'neill, B., Høj, P., & Jones, P.. (2005). Preventing protein haze in bottled white wine. *Australian Journal of Grape and Wine Research, 11*(2), 215–225. https://doi.org/10.1111/j.1755-0238.2005.tb00289.x

Wilkinson, K. L., Ristic, R., Szeto, C., Capone, D. L., Yu, L., & Losic, D. (2022). Novel use of activated carbon fabric to mitigate smoke taint in grapes and wine. *Australian Journal of Grape and Wine Research, 28*(3), 500–507. https://doi.org/10.1111/ajgw.12548